Supplementary Information (SI) for RSC Advances.

Up-converting β-$NaY_{0.8}[Yb_{0.18}Er_{0.02}]F_4$ nanoparticles coated by superparamagnetic γ-Fe_2O_3 nanosatellites: Elaboration, characterization and *in vitro* cytotoxicity

M. Parvizian,[a,b] W. Mnasri,[a,c] M. Pleckaitis,[b] V. Karabanovas,[b] H. Khan,[a] S. Nowak,[a] S. Gam-Derouich,[a] L. Ben Tahar,[c,d] O. Sandre,[e] R. Rotomskis,[b] S. Ammar[a,*]

[a] Université Paris Cité, ITODYS, CNRS UMR-7086, Paris 75205, France
[b] Biomedical Physics Laboratory, National Cancer Institute, Vilnius 08408, Lithuania
[c] Université de Carthage, Faculté des Sciences de Bizerte, LR18 ES11, Laboratoire CHO-MN, Zarzouna 7021, Tunisia
[d] Northern Borders University, College of Science, Department of Chemistry, 73213 Arar, Saudia Arabia.
[e.] Univ. Bordeaux, CNRS, Bordeaux INP, UMR-5629, LCPO, Pessac 33607, France.

Supporting information

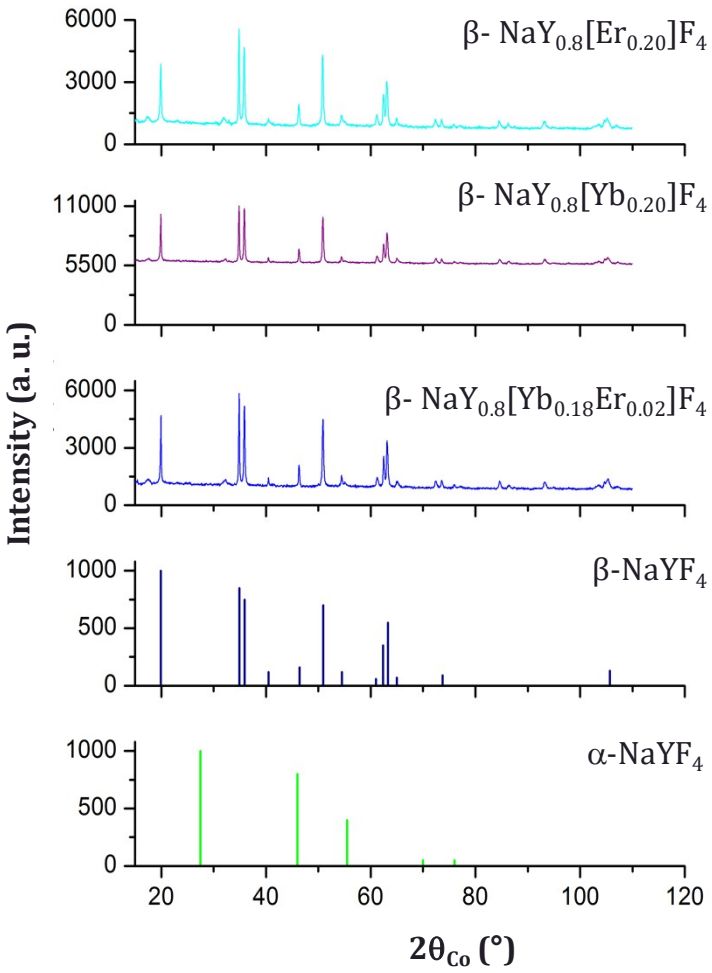

Figure S1. XRD patterns of the as-produced β-$NaY_{0.8}[Er_{0.2}]F_4$, β-$NaY_{0.8}[Yb_{0.2}]F_4$ and β-$NaY_{0.8}[Yb_{0.18}Er_{0.02}]F_4$ powders, recorded at room temperature and compared to those of tabulated cubic α-$NaYF_4$ (ICDD n°98-006-0257) and hexagonal β-$NaYF_4$ (ICDD n°98-005-1916) references.

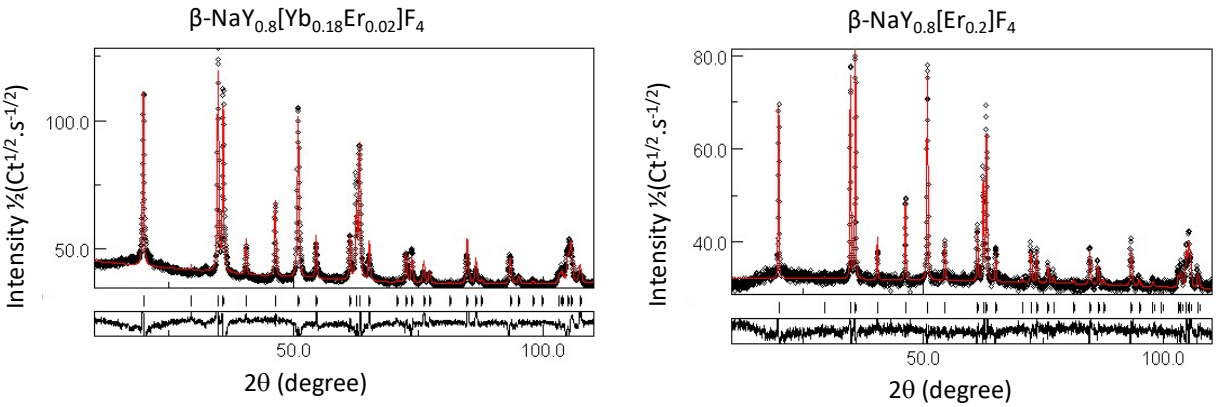

Figure S2. Experimental (black scatter) and calculated (red line) XRD patterns of β-$NaY_{0.8}[Yb_{0.18}Er_{0.02}]F_4$ (left) and β-$NaY_{0.8}[Erb_{0.2}]F_4$ (right). The residue, defined as the difference between the experimental and calculated diffractograms, is given separately, on the bottom of each graph. A pseudo-Voigt function was used for modelling the peak profile. A set of about 11 parameters was then refined, including the scale factor, the zero shift, the background polynomial coefficients, the peak profile parameters, and for the hexagonal fluoride phase, its cell parameters, average crystallographic coherence length (assuming isotropic crystals) and average lattice micro-deformation. The fitting was achieved with reliability Bragg factor R_B values close to 2.

	a / Å (*) ±0.002	*c* / Å (*) ±0.002	$<L_{XRD}>$ / nm ±2	$<\sqrt{\varepsilon^2}>$ %
β-$NaY_{0.8}[Yb_{0.18}Er_{0.02}]F_4$	5.970	3.511	98	<0.1
β-$NaY_{0.8}[Yb_{0.2}]F_4$	5.969	3.510	92	0.1
β-$NaY_{0.8}[Er_{0.2}]F_4$	5.975	3.513	95	<0.1

(*) Bulk β-$NaYF_4$ cell parameters a = 5.986 Å and c = 3.524 Å (ICDD n°98-005-1916)

Table S1. Unit cell parameters, mean crystallite size $<L_{XRD}>$ and average lattice micro-deformation $<\sqrt{\varepsilon^2}>$ determined by Rietveld analysis of the XRD pattern of the as-produced β-$NaY_{0.8}[Yb_{0.18}Er_{0.02}]F_4$, β-$NaY_{0.8}[Yb_{0.2}]F_4$ and β-$NaY_{0.8}[Er_{0.2}]F_4$.

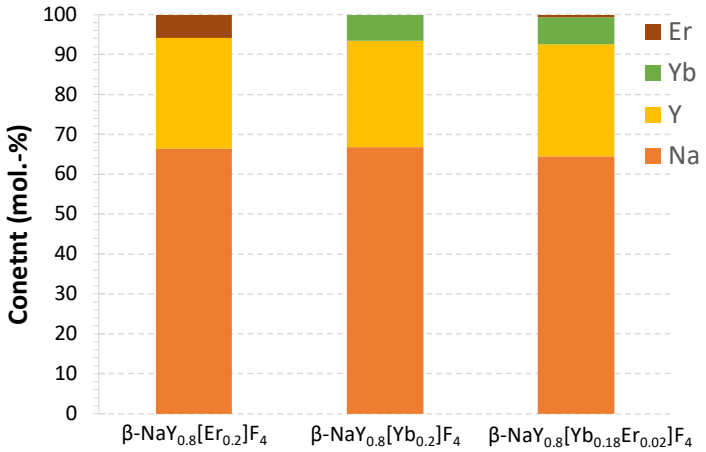

Figure S3. XRF chemical analysis of the as-produced β-$NaY_{0.8}[Er_{0.2}]F_4$, β-$NaY_{0.8}[Yb_{0.2}]F_4$ and β-$NaY_{0.8}[Yb_{0.18}Er_{0.02}]F_4$ powders.

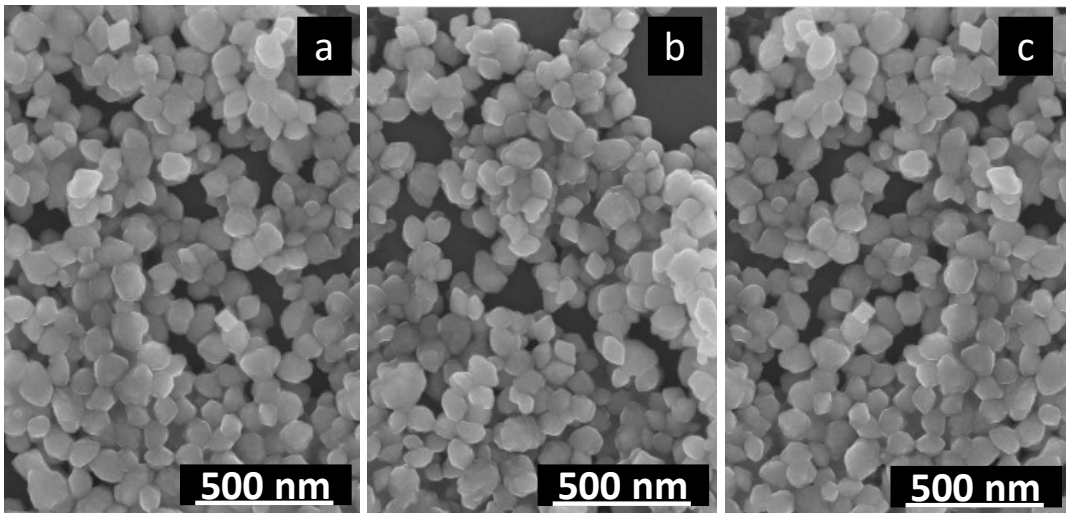

Figure S4. SEM Images recorded on the as-produced (a) β-$NaY_{0.8}[Er_{0.2}]F_4$, (b) β-$NaY_{0.8}[Yb_{0.2}]F_4$ and (c) β-$NaY_{0.8}[Yb_{0.18}Er_{0.02}]F_4$ powders.

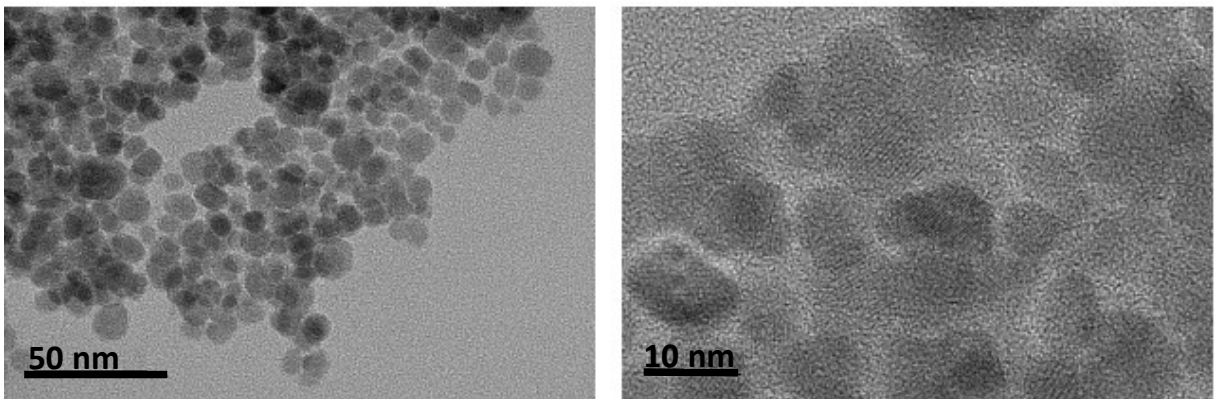

Figure S5. TEM Images, recorded at different magnifications, of an assembly of iron oxide nanoparticles prepared separately.

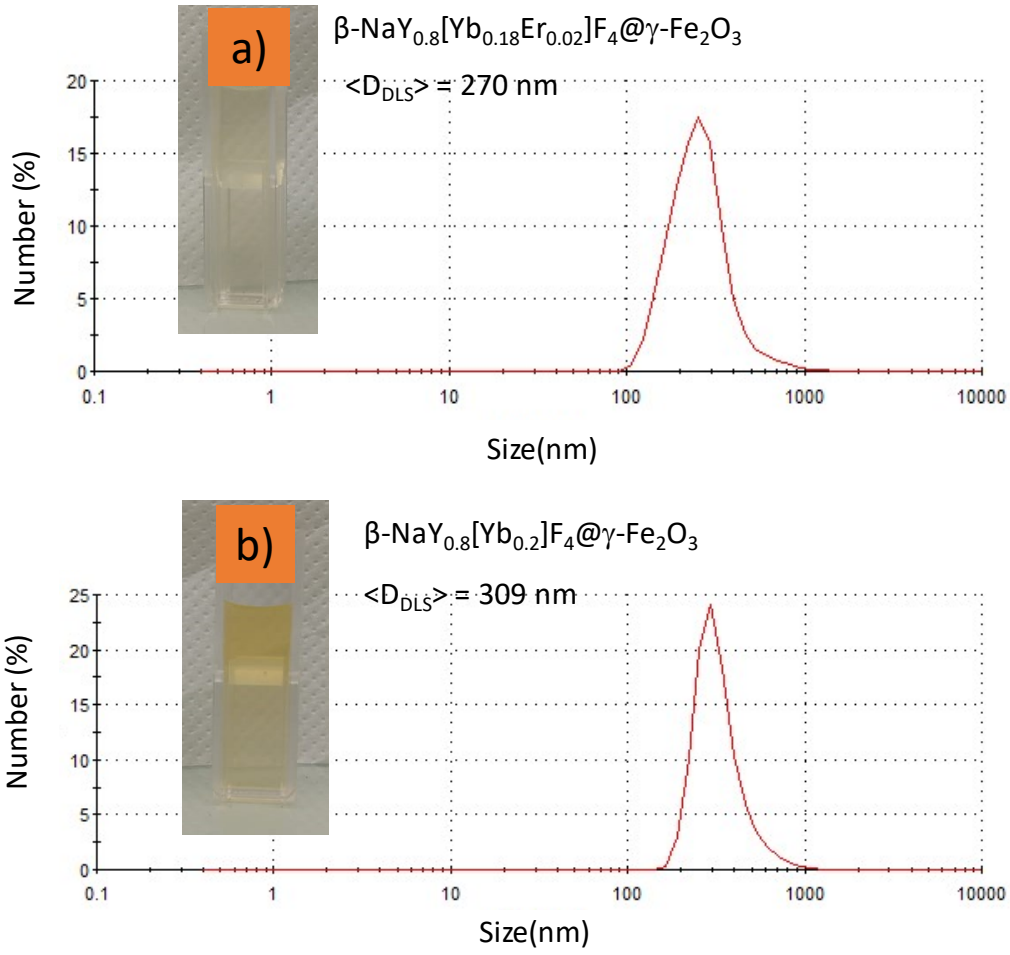

Figure S6. Hydrodynamic size distribution measured by DLS on the citrate treated (a) β-$NaY_{0.8}[Yb_{0.18}Er_{0.02}]F_4$@γ-$Fe_2O_3$ and (b) β-$NaY_{0.8}[Yb_{0.2}]F_4$@γ-Fe_2O_3 (lower graph) composite particles dispersed in milli-Q water. Numerical images of their aqueous colloids is given in the inset.

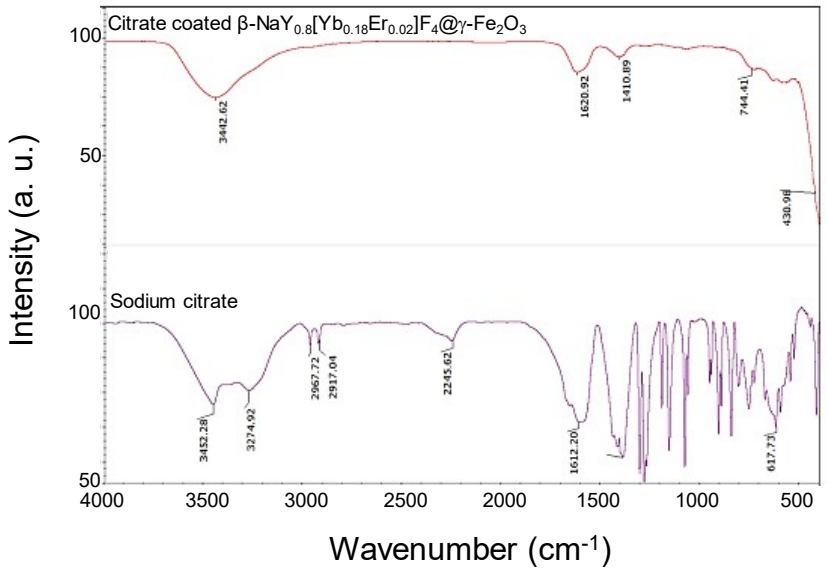

Figure S7. FTIR spectrum of citrate treated β-$NaY_{0.8}[Yb_{0.18}Er_{0.02}]F_4$@γ-$Fe_2O_3$ composite particles compared to that of sodium citrate salt.

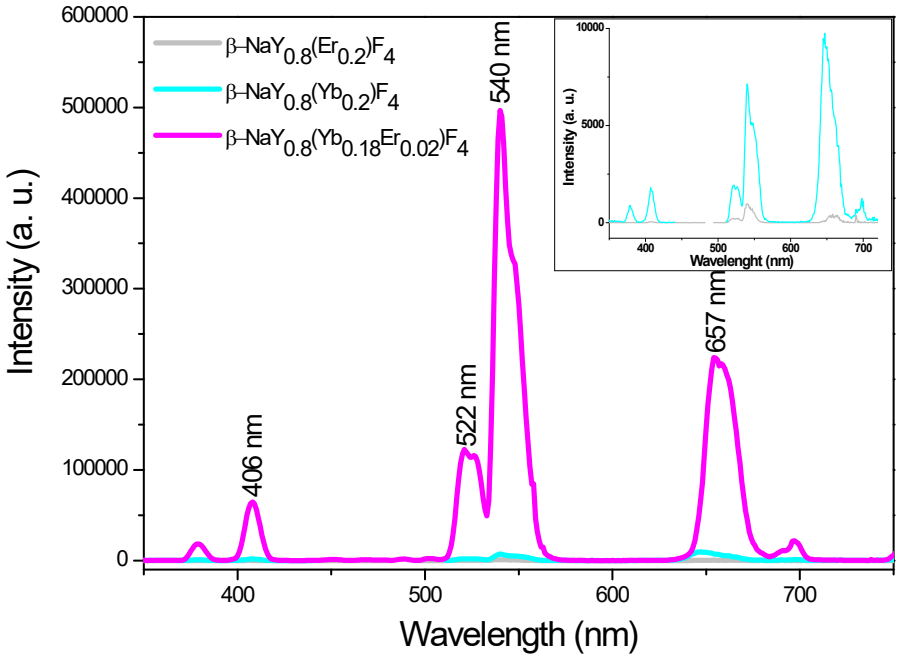

Figure S8. Emission spectra of β-$NaY_{0.8}[Er_{0.2}]F_4$ (grey line), β-$NaY_{0.8}[Yb_{0.2}]F_4$ (cyan line) and β-$NaY_{0.8}[Yb_{0.18}Er_{0.02}]F_4$ (magenta line) aqueous colloidal dispersion in water milli-Q (1 µg.mL^{-1}) recorded at r.t. under a laser irradiation of 980 nm at the day of preparation. A zoom of the spectra with the lowest intensity is given in the inset to highlight their fine structure.

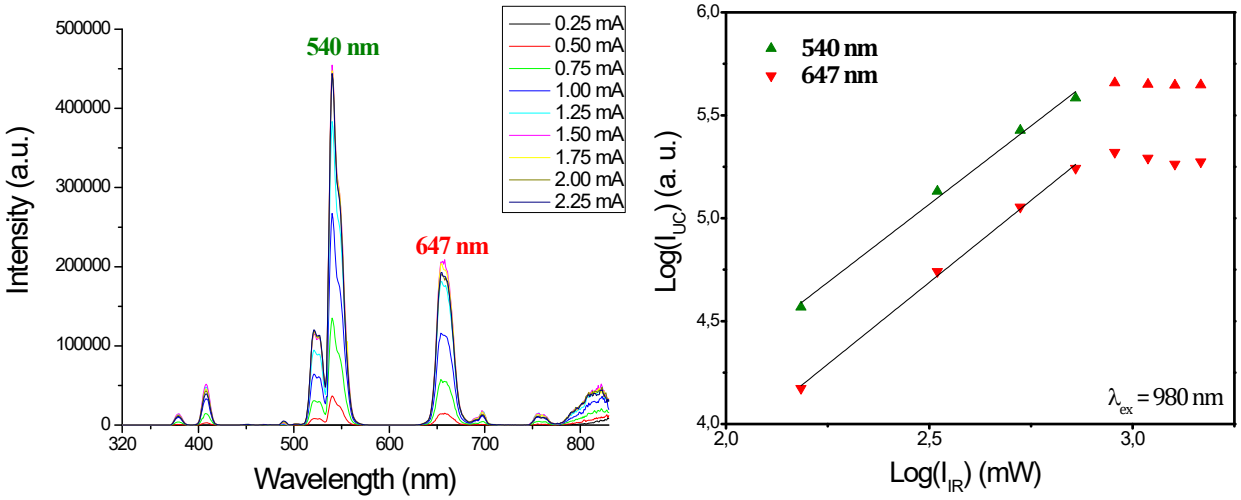

Figure S9. Emission spectra of β-$NaY_{0.8}[Yb_{0.18}Er_{0.02}]F_4$ aqueous colloidal dispersion in water milli-Q (1 µg.mL^{-1}) recorded at r.t. under a laser irradiation of 980 nm and various powers, the day of preparation. The emission intensity reached a maximum for a current laser alimentation of 1.00 mA. This value was chosen for the rest of the optical properties investigations.

a **b**

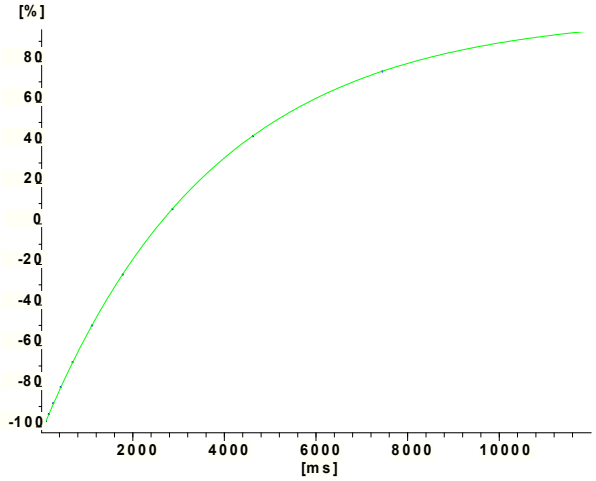
[%]
80
60
40
20
0
-20
-40
-60
-80
-100
2000
4000
6000
8000
10000
[ms]

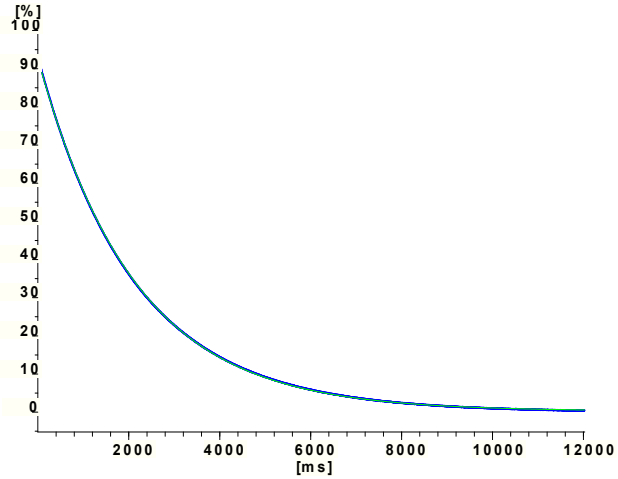
[%]
100
90
80
70
60
50
40
30
20
10
0
2000
4000
6000
8000
10000
12000
[ms]

c

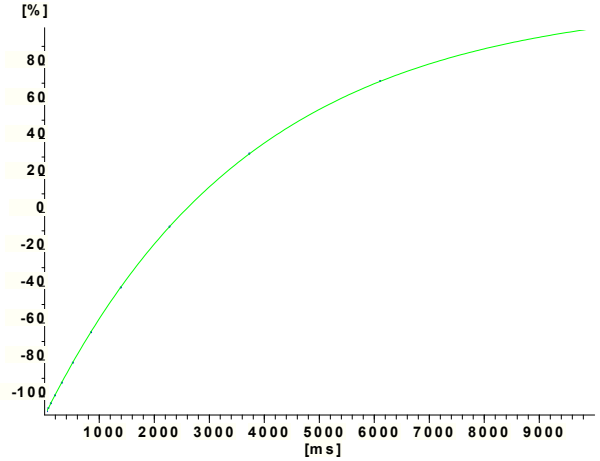
[%]
80
60
40
20
0
-20
-40
-60
-80
-100
1000
2000
3000
4000
5000
6000
7000
8000
9000
[ms]

d

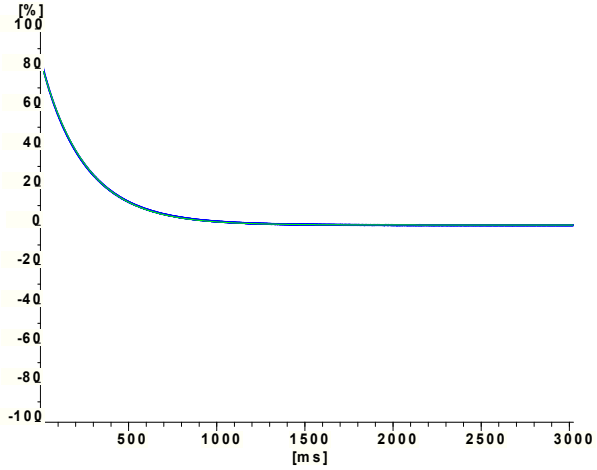
[%]
100
80
60
40
20
0
-20
-40
-60
-80
-100
500
1000
1500
2000
2500
3000
[ms]

e

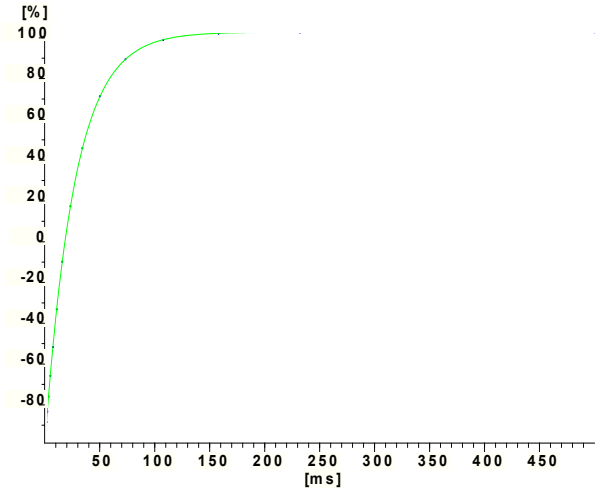
[%]
100
80
60
40
20
0
-20
-40
-60
-80
50
100
150
200
250
300
350
400
450
[ms]

f

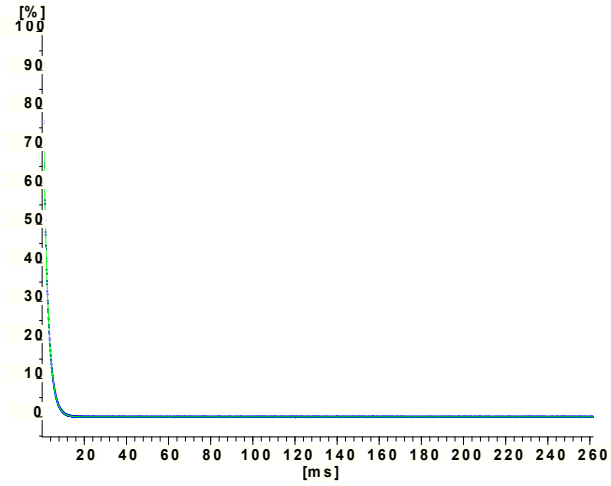
[%]
100
90
80
70
60
50
40
30
20
10
0
20
40
60
80
100
120
140
160
180
200
220
240
260
[ms]

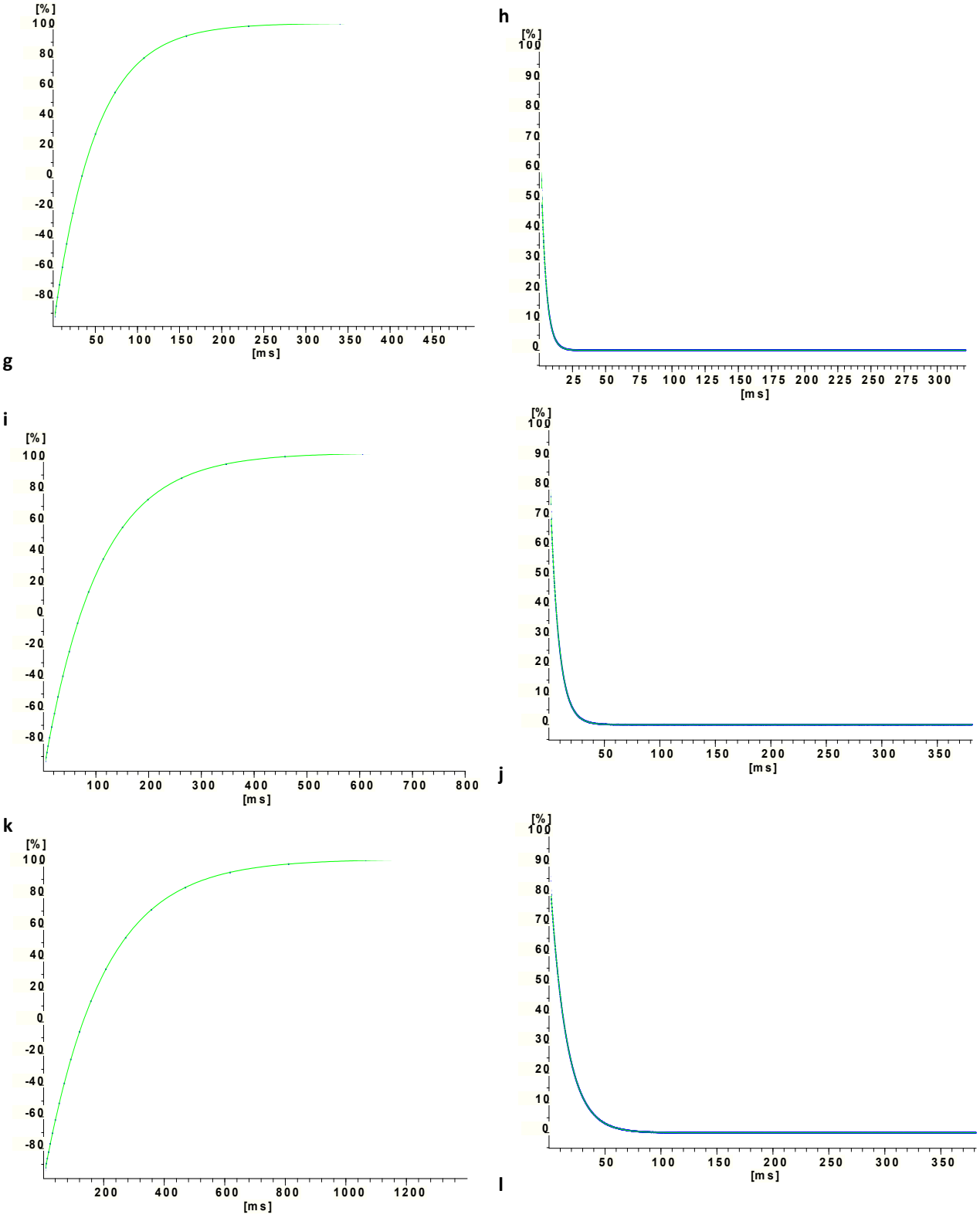

Figure S10. Examples of proton relaxation curves of respectively longitudinal (a, c, e, g, i, k) and transverse (b, d, f, h, j, l) nuclear magnetization, measured respectively by an inversion-recovery (IR) or a Carr-Purcell-Meiboom-Gill (CPMG) sequence on a Minispec mq60 relaxometer at different total magnetic metal concentrations: a, b) pure water (T_1=3740±10 ms, T_2=2126.8±0.6 ms) ; c, d) β-$NaY_{0.8}[Yb_{0.18}Er_{0.02}]F_4$ at [Er]= 25 µM (T_1=3549±10 ms, T_2=248±0.1 ms); e, f) β-$NaY_{0.8}[Yb_{0.18}Er_{0.02}]F_4$@γ-$Fe_2O_3$ at [Er]+[Fe]= 2.36 mM (T_1=27.22±0.02 ms, T_2=2.215±0.001 ms); g, h) β-$NaY_{0.8}[Yb_{0.18}Er_{0.02}]F_4$@γ-$Fe_2O_3$ at [Er]+[Fe]= 1.18 mM (T_1=49.68±0.02 ms, T_2=3.834±0.002 ms); i, j) β-

$NaY_{0.8}[Yb_{0.18}Er_{0.02}]F_4$@γ-$Fe_2O_3$ at [Er]+[Fe]= 0.59 mM (T_1=103.07±0.03 ms, T_2=7.855±0.002 ms); k, l) β-$NaY_{0.8}[Yb_{0.18}Er_{0.02}]F_4$@γ-$Fe_2O_3$ at [Er]+[Fe]= 0.295 mM (T_1=193.1±0.2 ms, T_2=14.867±0.003 ms).